Electronic structure and magnetic properties of monoclinic β-Cu$_2$V$_2$O$_7$: A GGA+U study

Masatomo Yashima[1,*] and Ryosuke O. Suzuki[2]

[1]*Department of Materials Science and Engineering, Interdisciplinary Graduate School of Science and Engineering,*
Tokyo Institute of Technology, Nagatsuta-cho 4259, Midori-ku, Yokohama, Kanagawa, 226-8502, Japan
[2]*Department of Material Science, Graduate School of Engineering, Hokkaido University, N13W8 Kita-ku, Sapporo, 060-8628, Japan*

A first-principles study on monoclinic $C2/c$ copper pyrovanadate β-Cu$_2$V$_2$O$_7$ has been performed using the generalized gradient approximation (GGA) and GGA+U method. The optimized unit-cell parameters and atomic coordinates of β-Cu$_2$V$_2$O$_7$ agree well with experimental data. The optimized crystal structure of β-Cu$_2$V$_2$O$_7$ indicates the existence of one-dimensional -Cu-Cu-Cu-Cu- chains. The electronic structure and magnetic properties were evaluated by the GGA+U calculations, which indicate that the β-Cu$_2$V$_2$O$_7$ is a semiconducting antiferromagnetic material with an indirect band gap and local magnetic moment per Cu atom of $0.73\mu_B$. The intrachain exchanges for short and long Cu-Cu couples are estimated to be 6.4 and 4.1 meV, respectively, while the calculated interchain exchange (2.1 meV) is smaller, which indicate the one-dimensional character. The top of the valence band is composed of V $3d$, O $2p$, and Cu $3d$ electrons while the bottom of the conduction band is primarily composed of Cu $3d$ electrons. Valence electron-density distribution map indicates the V-O and Cu-O covalent bonds. Calculated partial electronic density of states strongly suggests that the V-O and Cu-O covalent bonds are mainly attributed to the overlaps of V $3d$ and O $2p$ atomic orbitals and of Cu $3d$ and O $2p$, respectively.

PACS number(s): 71.20.Nr, 75.20.Hr

I. INTRODUCTION

One-dimensional (1D) spin systems have attracted a great deal of attention in condensed-matter physics due to their fascinating magnetic properties. In inorganic compounds containing Cu^{2+} ions ($3d^9$) or V^{4+} ions ($3d^1$), a number of quasi-1D spin systems such as CuGeO$_3$,[1] SrCuO,[2] (VO)$_2$P$_2$O$_7$,[3] and α'-NaVO (Ref. [4]) have extensively been studied. A variety of magnetic ground states in copper-based and/or vanadium-based oxides provide rich physics. In the present work we focus on the 1D system β-Cu$_2$V$_2$O$_7$.

The copper pyrovanadates Cu$_2$V$_2$O$_7$ exhibit interesting electrical, magnetic, thermoelectric, electrochemical, and catalytic properties.[5–15] In the oxidation of isobutane under anaerobic conditions, the Cu$_2$V$_2$O$_7$ showed high oxidizing activity.[14] Copper vanadate exhibited high catalytic activity in the oxidation of toluene.[15] The Cu$_2$V$_2$O$_7$ is an n-type semiconductor.[9] The Cu$_2$V$_2$O$_7$ has at least two polymorphisms of low-temperature orthorhombic blossite (α-Cu$_2$V$_2$O$_7$, space-group $Fdd2$) (Refs. [16–18]) and high-temperature monoclinic ziesite (β-Cu$_2$V$_2$O$_7$, space-group $C2/c$; Fig. 1).[19] The α-Cu$_2$V$_2$O$_7$ transforms into the β phase at 712 °C.[16,18,19] Other forms of γ-Cu$_2$V$_2$O$_7$ and β'-Cu$_2$V$_2$O$_7$ were reported recently.[20–22] A number of researchers have investigated the electrical, magnetic, and thermoelectric properties of β-(Cu,Zn)$_2$V$_2$O$_7$.[6,8–11] The (Cu,Zn)$_2$V$_2$O$_7$ solid solutions have large negative values of Seebeck coefficient.[9,10] The β-Cu$_2$V$_2$O$_7$ and β-(Cu,Zn)$_2$V$_2$O$_7$ have been regarded as a quasi-one-dimensional spin system composed of magnetic Cu^{2+} ions. In the present work, we focus on the end member β-Cu$_2$V$_2$O$_7$.

First-principles calculations are useful to evaluate the structural, electric, magnetic, and thermoelectric properties.[23–32] However, the crystal, magnetic, and electronic structures of Cu$_2$V$_2$O$_7$ have not been studied theoretically. The purpose of the present work is to evaluate the structural, electronic, and magnetic properties of monoclinic β-Cu$_2$V$_2$O$_7$ by the GGA+U method. The present study on the β-Cu$_2$V$_2$O$_7$ can be a good starting point to understand the structural, electronic, thermoelectric, and magnetic properties of the β-(Cu,Zn)$_2$V$_2$O$_7$ solid solutions. Our results clearly establish that the ground state of β-Cu$_2$V$_2$O$_7$ consists
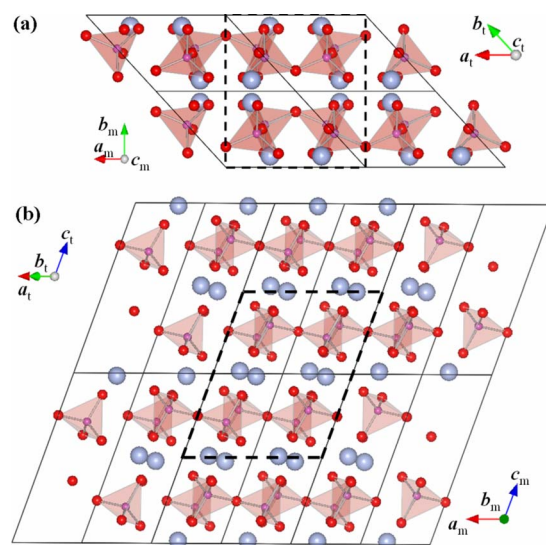

FIG. 1. (Color online) Crystal structure of monoclinic β-Cu$_2$V$_2$O$_7$ depicted with optimized crystallographic parameters. Views projected onto (a) (001) and (b) (010) planes. Gray (large), pink (small), and red (dark) spheres denote the Cu, V, and O atoms, respectively. Thick dashed lines denote the monoclinic $C2/c$ unit cell. Eight primitive unit cells ($2a_t \times 2b_t \times 2c_t$, space-group $P1$) are drawn with thin solid lines. Axes a_m, b_m, and c_m denote the directions of lattice vectors of the monoclinic cell. Axes a_t, b_t, and c_t denote the directions of lattice vectors of the triclinic primitive cell.

of magnetic Cu ions, which lead to an antiferromagnetic state. Furthermore the present GGA$+U$ calculations indicate that the β-Cu$_2$V$_2$O$_7$ is a semiconducting material with an indirect band gap.

II. COMPUTATIONAL DETAILS

The spin-polarized generalized gradient approximation (GGA) and GGA$+U$ method (U=on-site Coulomb repulsion strength, the so-called Hubbard U) electronic calculations were performed with Vienna *Ab initio* Simulation Package (VASP) (Ref. [24]) in order to obtain the valence electron-density distribution, density of states, and band structure in β-Cu$_2$V$_2$O$_7$. Calculations were performed using projector augmented-wave (PAW) potentials for Cu, V, and O atoms.[25] A plane-wave basis set with a cutoff of 500 eV was used. The Perdew-Burke-Ernzerhof GGA was employed for the exchange and correlation functionals. Sums over occupied electronic states were performed using the Monkhorst-Pack scheme[26] on a $3 \times 5 \times 3$ set of a k-point mesh. A simplified GGA$+U$ method after Dudarev *et al.*[32] was utilized. The value of U-J for β-Cu$_2$V$_2$O$_7$ (6.52 eV for Cu 3d channel) was adopted from the literature.[27,28]

Unit-cell parameters and atomic coordinates of β-Cu$_2$V$_2$O$_7$ were optimized with the convergence condition of 0.02 eV/Å for a primitive triclinic cell (Fig. 2) and a double triclinic cell (Fig. 3). Initial crystallographic parameters used in the optimization were referred from the literature.[16] To examine the effects of the Hubbard U on the calculation results, we also used the simple GGA method for the calculation of density of states (DOS). Wigner-Seitz radii for Cu, V, and O atoms were 1.17, 1.34, and 0.73 a.u., respectively, which were used in the calculations of local magnetic moments and partial atomic charges. Optimized crystal structure and its valence electron-density distribution were depicted with a computer program VESTA.[33]

III. RESULTS AND DISCUSSION

The crystal structure of β-Cu$_2$V$_2$O$_7$ is monoclinic as shown by the dashed lines in Fig. 1. We used the primitive triclinic cell of β-Cu$_2$V$_2$O$_7$ for the GGA$+U$ calculations (solid lines in Figs. 1 and 2). To examine the applicability and accuracy of both GGA$+U$ and the PAW methods, we first optimized the unit-cell parameters and atomic coordinates of β-Cu$_2$V$_2$O$_7$. The optimized crystallographic parameters corresponding to the lowest total energy are listed in Table I. Figures 1 and 2(a) show the optimized crystal and magnetic structures. The present calculated values exhibit good agreement with experimental data, which indicate the validity of GGA$+U$ method and PAW potentials used in this work. In the optimized crystal structure, one vanadium and four oxygen atoms form a VO$_4$ tetrahedron while a copper is coordinated with five oxygen atoms. The Cu-O bonds nearly perpendicular to the *b*-*c* plane have longer bond length (2.283 Å), compared with other Cu-O bonds on the *b*-*c* plane (1.925–1.966 Å). Here the *b* and *c* stand for the lattice vectors of the triclinic primitive cell. The longer Cu-O bond length is attributable to the Jahn-Teller distortion,[11,34]
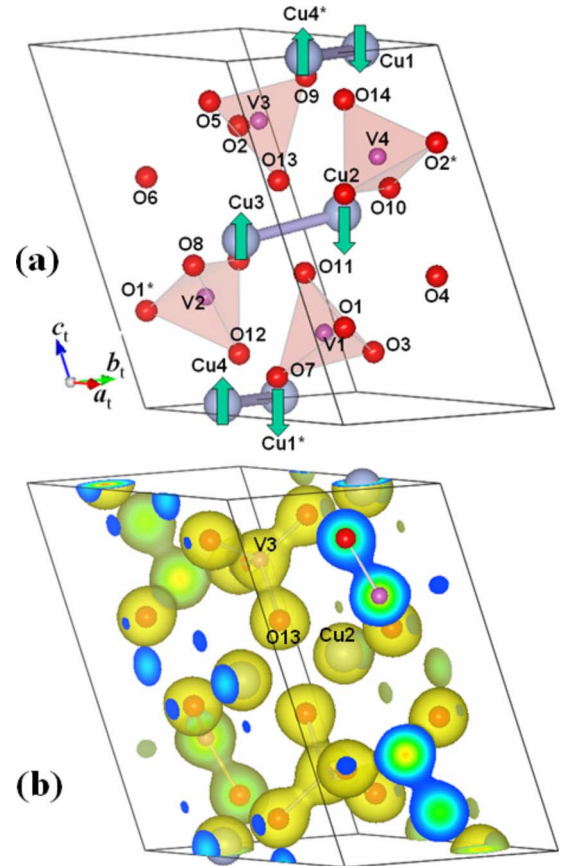

FIG. 2. (Color online) (a) Crystal structure of a primitive triclinic cell for monoclinic β-Cu$_2$V$_2$O$_7$ depicted with optimized crystallographic parameters of the antiferromagnetic ground state, which was obtained through GGA$+U$ calculations. (b) Isosurface at 0.8 Å^{-3} of corresponding valence electron density calculated by the GGA$+U$ method. Gray (large), pink (small), and red (dark) spheres denote the Cu, V, and O atoms, respectively. Thin lines denote the primitive cell. V-O bonds are drawn. Arrows at the Cu atoms denote the spin. Axes $\boldsymbol{a}_t$, $\boldsymbol{b}_t$, and $\boldsymbol{c}_t$ denote the directions of lattice vectors of the triclinic primitive cell. The atom with a star in Fig. 2(a) exists within a nearest-neighbor cell. Bonds between Cu and Cu atoms are drawn to show the Cu-Cu couple in Fig. 2(a).

which result in the elongated square-pyramidal CuO$_5$.

To investigate the magnetic properties of β-Cu$_2$V$_2$O$_7$, all possible magnetic moments corresponding to the ferromagnetic, antiferromagnetic, and nonmagnetic (paramagnetic) phases (Table II) were initially assigned to the four Cu atoms in the primitive unit cell [arrows in Fig. 2(a)]. Structural optimization and self-consistent convergence were performed for each initial setting. It was confirmed that the paramagnetic structure is unstable compared with the antiferromagnetic and ferromagnetic states. Total energy of the paramagnetic state is considerably (577 meV per Cu atom) higher than that of the antiferromagnetic ground state. On the contrary, total energies of the ferromagnetic and other antiferromagnetic phases are a little (4–9 meV per Cu atom) higher than that of the ground state. These results for β-Cu$_2$V$_2$O$_7$ are similar with those for CuO.[28]

It was found that the lowest energy, i.e., the ground state of the β-Cu$_2$V$_2$O$_7$ crystal, corresponds to the antiferromag-
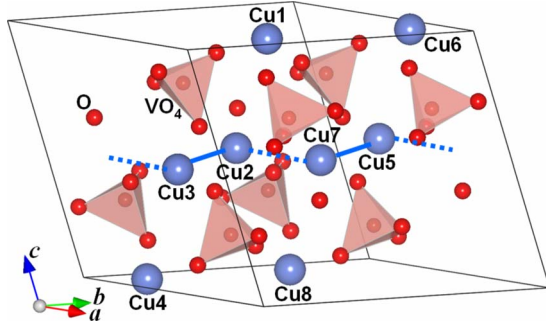
FIG. 3. (Color online) Crystal structure of a $1 \times 2 \times 1$ supercell (double primitive triclinic cell) for monoclinic β-Cu$_2$V$_2$O$_7$ depicted with optimized crystallographic parameters of the antiferromagnetic ground state, which was obtained through GGA+U calculations. Gray (large), pink (small), and red (dark) spheres denote the Cu, V, and O atoms, respectively. Thin lines denote the double primitive cell. Axes **a**, **b**, and **c** denote the directions of lattice vectors of the triclinic double primitive cell. Solid and dashed blue lines denote the short and long Cu-Cu bonds.

netic phase shown in Fig. 2(a) where the local magnetic moment per Cu atom is $0.73 \mu_B$ for Wigner-Seitz radius of 1.17 a.u. The antiferromagnetic phase found in the present calculations is consistent with the experimental study after Touaiher *et al.*[7] and after He and Ueda.[11] Based on the magnetic-susceptibility measurements, they concluded that the β-Cu$_2$V$_2$O$_7$ is antiferromagnetic. Touaiher *et al.*[7] suggested a magnetic model with two couples of copper ions. In our optimized structure model in Fig. 2(a), two couples of Cu1-Cu4 and Cu2-Cu3 exist. The interatomic distances between Cu2 and Cu3, and between Cu1 and Cu4 are short (2.9974 Å), which might stabilize this magnetic structure. The significantly reduced Cu^{2+} spin moment $0.73 \mu_B$ compared with μ_B expected for a Cu^{2+} ion is attributable to the covalent effect. Similarly reduced Cu^{2+} spin moment was also reported for copper oxide CuO.[35–39] Covalent bonds between Cu and O atoms are discussed later. The energy difference of intracouple [e.g., between Cu2(+)-Cu3(−) and Cu2(+)-Cu3(+)] is estimated to be E(Intra)=4.7 meV per one Cu-Cu intracouple from the Table II while that of inter-

TABLE I. Unit-cell parameters and atomic coordinates of monoclinic copper pyrovanadate β-Cu$_2$V$_2$O$_7$. Primitive triclinic cell shown in Figs. 1 and 2(a) is adopted.

	Experimental[a,b]	Theoretical (This work)
a (Å)	7.687	7.8468
b (Å)	5.54982	5.6213
c (Å)	10.09	10.18
α (deg)	104.00	103.61
β (deg)	110.45	109.71
γ (deg)	46.17	45.74
x, y, and z of Cu1 atom	0.7638, 0.8528, 0.9860	0.7582, 0.8522, 0.9841
x, y, and z of Cu2 atom	0.3834, 0.8528, 0.5140	0.3897, 0.8522, 0.5159
x, y, and z of Cu3 atom	0.6166, 0.1472, 0.4860	0.6103, 0.1478, 0.4841
x, y, and z of Cu4 atom	0.2362, 0.1472, 0.0140	0.2419, 0.1478, 0.0159
x, y, and z of V1 atom	0.5641, 0.4438, 0.2130	0.5566, 0.4431, 0.2134
x, y, and z of V2 atom	0.9921, 0.4438, 0.2870	0.0003, 0.4431, 0.2866
x, y, and z of V3 atom	0.4359, 0.5562, 0.7870	0.4434, 0.5569, 0.7866
x, y, and z of V4 atom	0.0079, 0.5562, 0.7130	0.9997, 0.5569, 0.7134
x, y, and z of O1 atom	0.8646, 0.2708, 0.2500	0.8650, 0.2700, 0.2500
x, y, and z of O2 atom	0.1354, 0.7292, 0.7500	0.1350, 0.7301, 0.7500
x, y, and z of O3 atom	0.3631, 0.8058, 0.1338	0.3673, 0.8110, 0.1354
x, y, and z of O4 atom	0.8311, 0.8058, 0.3662	0.8218, 0.8110, 0.3646
x, y, and z of O5 atom	0.6369, 0.1942, 0.8662	0.6327, 0.1890, 0.8646
x, y, and z of O6 atom	0.1689, 0.1942, 0.6338	0.1782, 0.1890, 0.6354
x, y, and z of O7 atom	0.5344, 0.1762, 0.1024	0.5339, 0.1805, 0.1021
x, y, and z of O8 atom	0.2894, 0.1762, 0.3976	0.2856, 0.1805, 0.3979
x, y, and z of O9 atom	0.4656, 0.8238, 0.8976	0.4661, 0.8195, 0.8979
x, y, and z of O10 atom	0.7106, 0.8238, 0.6024	0.7144, 0.8195, 0.6021
x, y, and z of O11 atom	0.4846,[b] 0.5024,[b] 0.3709	0.4853, 0.5046, 0.3723
x, y, and z of O12 atom	0.0130,[b] 0.5024,[b] 0.1291	0.0101, 0.5046, 0.1277
x, y, and z of O13 atom	0.5154,[b] 0.4976,[b] 0.6291	0.5147, 0.4954, 0.6277
x, y, and z of O14 atom	0.9870,[b] 0.4976,[b] 0.8709	0.9899, 0.4954, 0.8723

[a]Reference 16.
[b]Corrected coordinates are used. See Appendix for details.

TABLE II. The energy differences and total magnetic moment for the various magnetic phases in the primitive triclinic copper pyro-vanadate β-$Cu_2V_2O_7$ unit cell. The zero point of the energy is chosen as the ground-state antiferromagnetic configuration whose magnetic moments are indicated by the arrows in Fig. 2.

Magnetic configuration	Initial magnetic moment for each of the four Cu atoms				Energy difference per Cu atom (meV)	Total magnetic moment (μ_B)
	Cu1	Cu2	Cu3	Cu4		
Antiferromagnetic (Ground states)	−	−	+	+	0	0
Other antiferromagnetic states	+	−	+	−	4	0
	+	−	−	+	6	0
Paramagnetic state	0	0	0	0	577	0
Ferromagnetic states	+	+	+	+	9	4
	+	+	+	−	5	2

couple [e.g., between Cu1(−)-Cu2(−) and Cu1(+)-Cu2(−)] is 2.1 meV. There exist long and short Cu-Cu intracouples as shown by the blue solid and dot lines, respectively, in Fig. 3. To estimate the exchange constant for each Cu-Cu couple, structural optimization was performed for three antiferro-magnetic configurations with the double primitive cell (Fig. 3 and Table III). The exchange constants for the short and long Cu-Cu intracouples are calculated to be $E(\text{Intra Short})=6.4$ meV and $E(\text{Intra Long})=4.1$ meV, respectively. The ratio $2E(\text{Inter})/\{E(\text{Intra Short})+E(\text{Intra Long})\}=0.400$ is a little higher than the experimental data (0.354) in the literature.[11] The ratio value 0.4 clearly indicates that the β-$Cu_2V_2O_7$ compound has one-dimensional character.

Figures 4 and 5 show parts of the total DOS and band structure for the ground state of β-$Cu_2V_2O_7$ calculated using the GGA+U method (red solid lines in Fig. 4). To examine the effects of the Hubbard U on the calculation results, we also used the simple GGA method for the calculation of DOS using the same crystallographic parameters and energy cut-offs (blue dotted lines in Fig. 4). The symmetric DOS for both spin up and spin down indicates an antiferromagnetic state, which is consistent with the local magnetic-moment results in Fig. 2(a). The DOS calculated from the simple GGA method exhibits a metallic character while the GGA+U approach leads to a different picture of the DOS of β-$Cu_2V_2O_7$, with zero DOS at the Fermi level and an indirect band gap of 2.0 eV (Figs. 4 and 5). Therefore, by introducing the Hubbard U, the GGA+U calculations predict β-$Cu_2V_2O_7$ to be a semiconductor. This is consistent with

the experimental results after Sotojima *et al.*[9] where the electrical conductivity of β-$(Cu,Zn)_2V_2O_7$ and α-$Cu_2V_2O_7$ decreases with increasing temperature.

Figure 6 shows parts of partial density of states (PDOS) for V3, O13, and Cu2 atoms. The top of the valence band is composed of V 3d, O 2p, and Cu 3d electrons. The bottom of the conduction band is primarily composed of Cu 3d electrons. Figure 2(b) shows the isosurface of the valence electron density of β-$Cu_2V_2O_7$ at 0.8 Å^{-3} obtained by the GGA+U calculations. Covalent bonds between the V and O atoms are clearly shown in Fig. 2(b), which are ascribed to the overlap of V 3d and O 2p atomic orbitals (Fig. 6).

The β-$Cu_2V_2O_7$ and β-$(Cu,Zn)_2V_2O_7$ have been regarded as a quasi-one-dimensional spin system composed of magnetic Cu^{2+} ions. Figure 7(a) indicates the one-dimensional -Cu3-Cu2-Cu3-Cu2- chain along the $\boldsymbol{b}_t$ axis in the optimized structure of β-$Cu_2V_2O_7$. The $\boldsymbol{b}_t$ denotes the lattice vector of the triclinic cell of β-$Cu_2V_2O_7$. There exist shorter Cu2-Cu3 (2.997 Å) and longer Cu2-Cu3 (3.242 Å) couples. Components of atomic partial charge for Cu s, p, and d orbitals were calculated to be 0.242, 0.251, and 8.931, respectively, which indicate the 3d^9 configuration. Figure 7(b) clearly shows the covalent bonds between the Cu and O atoms. The covalency is mainly attributable to the Cu 3d and O 2p atomic orbitals (Fig. 6). The covalency of the Cu^{2+} ions can be responsible for the significantly reduced Cu^{2+} spin moment 0.73μ_B compared with μ_B expected for a Cu^{2+} ion. The electron density at the middle point of the shorter Cu2-O13 bond is higher than that of the longer Cu2-O10 bond.

TABLE III. The energy differences and total magnetic moment for three magnetic phases in the double primitive triclinic copper pyrovanadate β-$Cu_2V_2O_7$ cell (Fig. 3). The zero point of the energy is chosen as the ground-state antiferromagnetic configuration.

Magnetic configuration	Initial magnetic moment for each of the four Cu atoms								Energy difference per Cu atom (meV)	Total magnetic moment (μ_B)
	Cu1	Cu2	Cu3	Cu4	Cu5	Cu6	Cu7	Cu8		
Antiferromagnetic[a] (Ground states)	−	−	+	+	−	−	+	+	0	0
Other antiferromagnetic states	−	−	+	+	+	+	−	−	4.1	0
	+	+	+	+	−	−	−	−	6.4	0

[a]Ground state in the double cell of this table is equivalent to that in the primitive one of Table II.
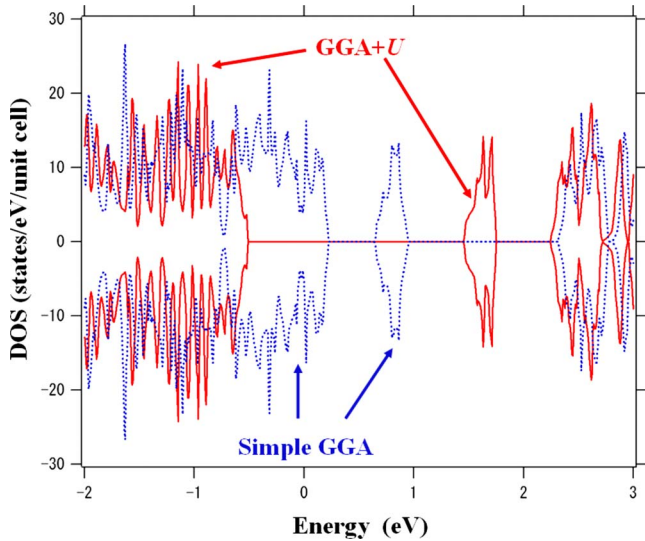
FIG. 4. (Color online) Comparison of density of states of a primitive triclinic cell for monoclinic β-$Cu_2V_2O_7$ from standard GGA (blue dotted lines) and GGA+U (red solid lines) calculations. The positive and negative DOS denote spin up and spin down, respectively. The energy zero point is chosen at Fermi level in the standard GGA calculation.

FIG. 6. (Color online) PDOS of d (blue line), p (red line), and s (green line but negligible) orbitals of Cu2, O13, and V3 atoms in monoclinic β-$Cu_2V_2O_7$. Atomic sites with numbers are referred from Fig. 2(a). The positive and negative PDOSs denote spin up and spin down, respectively.

IV. CONCLUSIONS

Crystal, magnetic, and electronic structures of monoclinic $C2/c$ copper pyrovanadate β-$Cu_2V_2O_7$ were evaluated by first-principles calculations for the first time. The optimized unit-cell parameters and atomic coordinates of β-$Cu_2V_2O_7$ agree well with experimental data. The elongated Cu-O bond nearly perpendicular to the **b-c** plane, which is attributable to the Jahn-Teller distortion, was confirmed in the optimized crystal structure of β-$Cu_2V_2O_7$. In addition, we corrected the

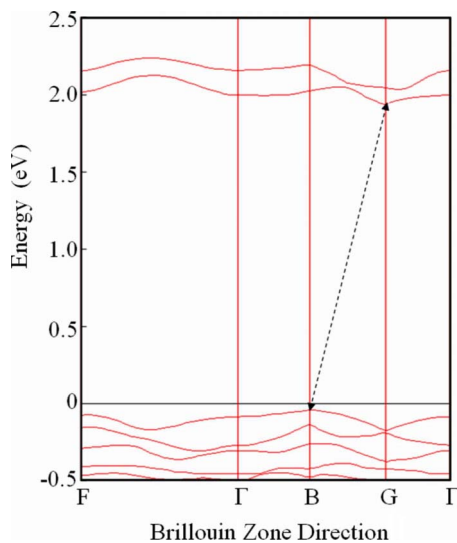FIG. 5. (Color online) A part of band structure of monoclinic β-$Cu_2V_2O_7$ from GGA+U calculations. The Fermi level (horizontal solid line) is set at 0 eV. Dashed line with arrows indicates the indirect band gap of 2.0 eV.
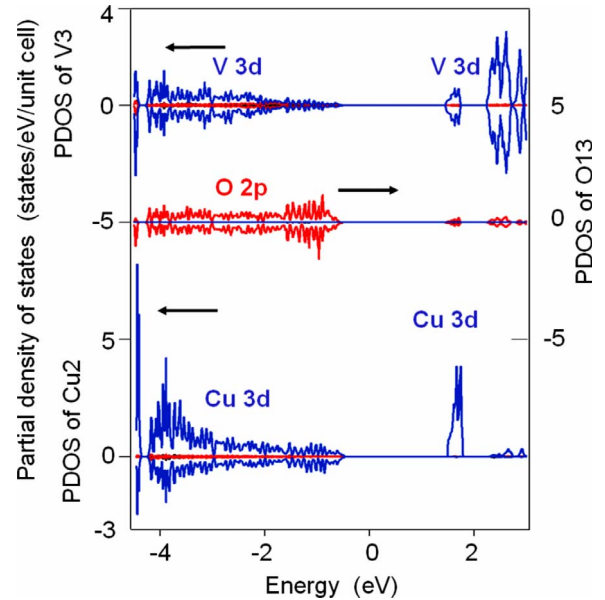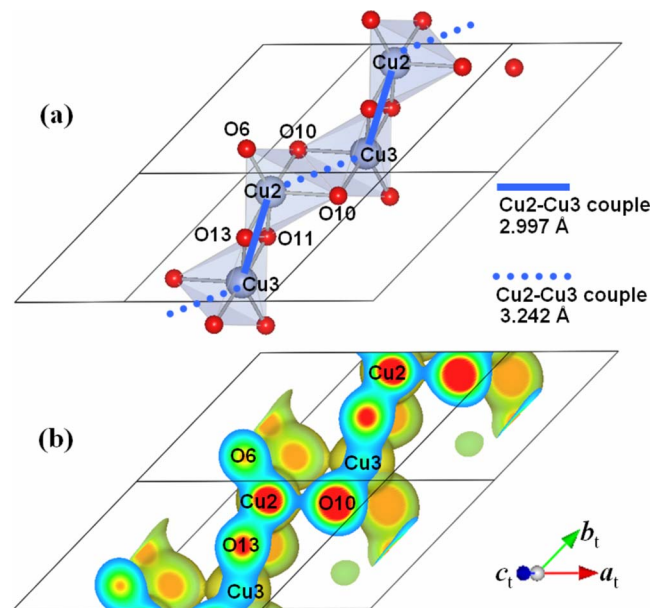

FIG. 7. (Color online) (a) Crystal structure and (b) corresponding isosurface of electron density at 0.25 Å^{-3} in β-$Cu_2V_2O_7$ depicted with optimized crystallographic parameters of the antiferromagnetic ground state, which was obtained through GGA+U calculations ($0 < x < 1$, $0 < y < 2$, $0.35 < z < 0.57$). Gray (large) and red (dark) spheres denote the Cu and O atoms, respectively. Thin lines denote the primitive cell. Structure in (a) is depicted with the elongated square-pyramidal CuO_5. Axes a_t, b_t, and c_t denote the directions of lattice vectors of the triclinic primitive cell. The blue solid and dotted lines are Cu2-Cu3 couples with the distances of 2.997 and 3.242 Å, respectively.

atomic coordinate y(O4) reported in the literature[16] (see Appendix). The GGA+U calculations indicate that the β-Cu$_2$V$_2$O$_7$ is a semiconducting antiferromagnetic material with an indirect band gap and local magnetic moment per Cu atom of $0.73\mu_B$ for Wigner-Seitz radius of 1.17 a.u. The intrachain exchanges for short and long Cu-Cu couples are estimated to be 6.4 and 4.1 meV, respectively, while the calculated interchain exchange (2.1 meV) is smaller, which indicate the one-dimensional character. The calculated PDOS indicates that the top of the valence band is composed of V 3d, O 2p, and Cu 3d electrons while the bottom of the conduction band is primarily composed of Cu 3d electrons. Covalent bonds between V and O atoms are mainly attributable to the overlap of V 3d and O 2p atomic orbitals. Covalent bonds between Cu and O atoms are mainly ascribed to the overlap of Cu 3d and O 2p. The covalence of Cu ions can be responsible for the significantly reduced Cu^{2+} spin

moment $0.73\mu_B$ compared with μ_B expected for a Cu^{2+} ion.

APPENDIX

Calvo and Faggiani[16] refined the crystal structure of monoclinic β-Cu$_2$V$_2$O$_7$ and reported the refined atomic coordinate y of O4 atom to be y(O4)=0.7152. This value is incorrect and the correct y(O4) value should be 0.7512. The reported value $[y$(O4)=0.7152$]$ yields a different Cu-O4 interatomic distance of 0.2167(5) Å from the value 0.1950(5) Å reported in the same paper.[16] On the contrary, the new value $[y$(O4)=0.7512$]$ makes the same value 0.1950(5) Å. The reported coordinate $[y$(O4)=0.7152$]$ is not consistent with the theoretical value obtained through the present GGA+U calculations but the corrected coordinate y(O4)=0.7512 is consistent with the theoretical value (Table I).

*Corresponding author; yashima@materia.titech.ac.jp

[1] M. Hase, I. Terasaki, and K. Uchinokura, Phys. Rev. Lett. **70**, 3651 (1993).

[2] M. Azuma, Z. Hiroi, M. Takano, K. Ishida, and Y. Kitaoka, Phys. Rev. Lett. **73**, 3463 (1994).

[3] T. Barnes and J. Riera, Phys. Rev. B **50**, 6817 (1994).

[4] M. Isobe and Y. Ueda, J. Phys. Soc. Jpn. **65**, 1178 (1996).

[5] L. A. Ponomarenko, A. N. Vasil'ev, E. V. Antipov, and Yu. A. Velikodny, Physica B **284-288**, 1459 (2000).

[6] J. Pommer, V. Kataev, K.-Y. Choi, P. Lemmens, A. Ionescu, Yu. Pashkevich, A. Freimuth, and G. Güntherodt, Phys. Rev. B **67**, 214410 (2003).

[7] M. Touaiher, K. Rissouli, K. Benkhouja, M. Taibi, J. Aride, A. Boukhari, and B. Heulin, Mater. Chem. Phys. **85**, 41 (2004).

[8] V. Kataev, J. Pommer, K.-Y. Choi, P. Lemmens, A. Ionescu, Yu. Pashkevich, K. Lamonova, A. Möller, A. Freimuth, and G. Güntherodt, J. Magn. Magn. Mater. **272-276**, 933 (2004).

[9] K. Sotojima, R. O. Suzuki, K. Amezawa, and Y. Tomii, Mater. Trans. **48**, 2094 (2007).

[10] K. Sotojima, R. O. Suzuki, K. Amezawa, and Y. Tomii, J. Jpn. Soc. Powder Powder Metall. **54**, 356 (2007).

[11] Z. He and Y. Ueda, Phys. Rev. B **77**, 052402 (2008).

[12] Y. Sakurai, H. Ohtsuka, and J. Yamaki, J. Electrochem. Soc. **135**, 32 (1988).

[13] C. Resini, F. Milella, and G. Busca, Phys. Chem. Chem. Phys. **2**, 2039 (2000).

[14] S. Hikazudani, K. Kikutani, K. Nagaoka, T. Inoue, and Y. Takita, Appl. Catal., A **345**, 65 (2008).

[15] L. A. Palacio, E. R. Silva, R. Catalão, J. M. Silva, D. A. Hoyos, F. R. Ribeiro, and M. F. Ribeiro, J. Hazard. Mater. **153**, 628 (2008).

[16] C. Calvo and R. Faggiani, Acta Crystallogr., Sect. B: Struct. Crystallogr. Cryst. Chem. **31**, 603 (1975).

[17] P. D. Robinson, J. M. Hughes, and M. L. Malinconico, Am. Mineral. **72**, 397 (1987).

[18] D. Mercurio-Lavaud and M. B. Frit, Acta Crystallogr., Sect. B: Struct. Crystallogr. Cryst. Chem. **29**, 2737 (1973).

[19] D. Mercurio-Lavaud and M. B. Frit, C. R. Acad. Sci. Paris

C277, 1101 (1973).

[20] G. M. Clark and R. Garlick, J. Inorg. Nucl. Chem. **40**, 1347 (1978).

[21] S. V. Krivovichev, S. K. Filatov, P. N. Cherepansky, T. Armbruster, and O. Y. Pankratova, Can. Mineral. **43**, 671 (2005).

[22] S. A. Petrova, R. G. Zakharov, M. V. Rotermel', T. I. Krasnenko, and N. A. Vatolin, Dokl. Akad. Nauk **400**, 770 (2005).

[23] M. Yashima, K. Fukuda, Y. Tabira, and M. Hisamura, Chem. Phys. Lett. **451**, 48 (2008).

[24] G. Kresse and D. Joubert, Phys. Rev. B **59**, 1758 (1999).

[25] J. P. Perdew, K. Burke, and M. Ernzerhof, Phys. Rev. Lett. **77**, 3865 (1996).

[26] H. J. Monkhorst and J. D. Pack, Phys. Rev. B **13**, 5188 (1976).

[27] V. I. Anisimov, J. Zaanen, and O. K. Andersen, Phys. Rev. B **44**, 943 (1991).

[28] D. Wu, Q. Zhang, and M. Tao, Phys. Rev. B **73**, 235206 (2006).

[29] M. Yashima, Y. Lee, and K. Domen, Chem. Mater. **19**, 588 (2007).

[30] M. Yashima, Y. Ando, and Y. Tabira, J. Phys. Chem. B **111**, 3609 (2007).

[31] M. Yashima, K. Ogisu, and K. Domen, Acta Crystallogr., Sect. B: Struct. Sci. **B64**, 291 (2008).

[32] S. L. Dudarev, G. A. Botton, S. Y. Savrasov, C. J. Humphreys, and A. P. Sutton, Phys. Rev. B **57**, 1505 (1998).

[33] K. Momma and F. Izumi, J. Appl. Crystallogr. **41**, 653 (2008).

[34] M. Schindler and F. C. Hawthorne, J. Solid State Chem. **146**, 271 (1999).

[35] T. Shimizu, T. Matsumoto, A. Goto, T. V. Chandrasekhar Rao, K. Yoshimura, and K. Kosuge, Phys. Rev. B **68**, 224433 (2003).

[36] B. X. Yang, J. M. Tranquada, and G. Shirane, Phys. Rev. B **38**, 174 (1988).

[37] J. B. Forsyth, P. J. Brown, and B. M. Wanklyn, J. Phys. C **21**, 2917 (1988).

[38] B. X. Yang, T. R. Thurston, J. M. Tranquada, and G. Shirane, Phys. Rev. B **39**, 4343 (1989).

[39] J. W. Loram, K. A. Mirza, C. P. Joyce, and A. J. Osborne, Europhys. Lett. **8**, 263 (1989).